condensed matter

MDPI

Article

Tuning the Electrical Parameters of p-NiO_x-Based Thin Film Transistors (TFTs) by Pulsed Laser Irradiation

Poreddy Manojreddy [1], Srikanth Itapu [2,*], Jammalamadaka Krishna Ravali [3] and Selvendran Sakkarai [4]

1 Department of ECE, CVR College of Engineering, Rangareddy 501510, India; manojreddy0359@gmail.com
2 Department of Sensors & Biomedical Technology, School of Electronics Engineering (SENSE), Vellore Institute of Technology (VIT), Vellore 632014, India
3 School of MS, University of Hyderabad, Hyderabad 500032, India; 19mbmb12@uohyd.ac.in
4 School of Electronics Engineering (SENSE), Vellore Institute of Technology Chennai Campus, Chennai 600127, India; selvendrans@aol.com
* Correspondence: srikanth.itapu@rockets.utoledo.edu

Abstract: We utilized laser irradiation as a potential technique in tuning the electrical performance of NiO_x/SiO_2 thin film transistors (TFTs). By optimizing the laser fluence and the number of laser pulses, the TFT performance was evaluated in terms of mobility, threshold voltage, on/off current ratio and subthreshold swing, all of which were derived from the transfer and output characteristics. The 500 laser pulses-irradiated NiO_x/SiO_2 TFT exhibited an enhanced mobility of 3 cm^2/V-s from a value of 1.25 cm^2/V-s for as-deposited NiO_x/SiO_2 TFT, subthreshold swing of 0.65 V/decade, on/off current ratio of 6.5×10^4 and threshold voltage of -12.2 V. The concentration of defect gap states as a result of light absorption processes explains the enhanced performance of laser-irradiated NiO_x. Additionally, laser irradiation results in complex thermal and photo thermal changes, thus resulting in an enhanced electrical performance of the p-type NiO_x/SiO_2 TFT structure.

Keywords: laser irradiation; p-type NiO; SiO_2 layer; thin film transistor

Citation: Manojreddy, P.; Itapu, S.; Ravali, J.K.; Sakkarai, S. Tuning the Electrical Parameters of p-NiO_x-Based Thin Film Transistors (TFTs) by Pulsed Laser Irradiation. *Condens. Matter* **2021**, *6*, 21. https://doi.org/10.3390/condmat6020021

Received: 14 March 2021
Accepted: 10 June 2021
Published: 11 June 2021

Publisher's Note: MDPI stays neutral with regard to jurisdictional claims in published maps and institutional affiliations.

Copyright: © 2021 by the authors. Licensee MDPI, Basel, Switzerland. This article is an open access article distributed under the terms and conditions of the Creative Commons Attribution (CC BY) license (https://creativecommons.org/licenses/by/4.0/).

1. Introduction

Metal oxide semiconductors have been widely used for applications in thin-film transistors (TFTs), gas sensors and carrier transporting layers in solar cells due to their defect engineering capabilities [1]. Extensive research on n-type oxide semiconductors [for example, Indium Gallium Zinc Oxide (InGaZnO), Zinc Oxide (ZnO) and Indium Oxide (In_2O_3)] resulted in industry-specific high-performance oxide TFTs. It is imperative to develop p-type substitutes for the development of next-generation transparent electronics which can accentuate next-generation Complementary Metal Oxide Semiconductor (CMOS) circuits [2,3]. Few p-type semiconductors such as the compounds Tin Oxide (SnO), Copper Oxide (Cu_xO) and Nickel Oxide (NiO_x) were reported to have a reasonable electrical performance as p-type channels. High-performance n-type equivalent p-type oxides still remain challenging due to the deep valence band maximum (~6.5 eV) [4]. It is well known that stoichiometric deviation alters the electronic structure, and oxygen vacancy causes the formation of sub-gap defects and donor states in many oxides. Therefore, a trade-off between the stoichiometry and the mechanisms employed for defect termination processes is to determine the extent of tuning of the behavior of p-type TFTs.

NiO_x is a particularly interesting and promising material due to its wide range of applicability vis-à-vis rectifying diodes [5], p-type Metal Insulator Semiconductor (MIS) structures [6], tin whisker growth mitigation by NiO sublayers [7], etc. The stoichiometric NiO is a Mott insulator with a conductivity of 10^{-13} S/cm, while nonstoichiometric NiO_x is a wide-band-gap p-type semiconductor [8]. Several methods have been used for growing NiO films, including sputtering [9–12], e-beam evaporation [13,14], the chemical and plasma-enhanced chemical vapor method [15], sol-gel [16], pulsed laser deposition [17]

and spray pyrolysis [18,19]. Sputtering, which is a type of physical vapor deposition technique, is preferred due to its industrial scalability. Indeed, the sputter-deposited NiO_x films often exhibit a varied electrical conductivity [20,21]. Defect engineering is not well-established in O-rich NiO films [22]. Some recent studies used working gas and thermal annealing as viable techniques for interstitial/defect changes. However, the dynamics of interstitials/vacancies created due to laser irradiation are little discussed regarding non-stoichiometric NiO films [23].

In continuation of the previous work in [23], laser irradiation was also employed to study its effects in modifying the intrinsic properties of metallic [24,25], semiconducting [26–29], superconducting [30], multiferroic [31] and ceramic [32] thin films. In [33], the most frequently used high dielectric material, hafnium oxide (HfO_2), was subjected to irradiation by a continuous wave laser with a wavelength of 355 nm to analyze the temporal behavior of absorption annealing. In [34], the postdeposition annealing of tin oxide (SnO_2) thin films by ultra-short laser pulses resulted in a change in the refractive index and conductivity of the films. A significant modification in the stoichiometry, desorption of dopant atoms and adsorption of hydrogen atoms from the atmosphere were also observed. The crystallization of amorphous titanium oxide (TiO_2) by pulsed laser irradiation using an excimer laser is studied in [35]. Cadmium oxide (CdO) thin films deposited by the sol-gel coating method were laser-irradiated using a Q-switched Nd:YAG laser operating at its first and second harmonic wavelengths in [36]. An agglomeration of nanoparticles and a variation in the bandgap, photoluminescence spectra with laser irradiation were observed. The structural, optical, luminescent and vibrational properties of zinc oxide (ZnO) under the influence of continuous-wave CO_2 laser irradiation were studied in [37]. In this work, we explore the effect of ultra-violet (UV) laser irradiation in tuning the properties of NiO thin films, thus enhancing the electrical performance of NiO-based TFTs.

In [38], the low-temperature solution-processed p-type nickel oxide thin films along with the aluminum oxide Al_2O_3 gate dielectric significantly improved the electrical performance of NiO_x TFT compared to the SiO_2-based dielectric. The hole mobility was reportedly enhanced to 4.4 cm^2/Vs. Similarly, ink-jet printed p-type NiO_x TFTs annealed at 280 °C in [39] gave the best electrical performance with a field-effect mobility of 0.78 cm^2/Vs, SS of 1.68 V/dec, on/off current ratio (I_{on}/I_{off}) of 5.3×10^4 with a 50 nm Al_2O_3 insulator layer. The authors in [40] successfully achieved p-type NiO TFTs with a mobility of 6.0 cm^2/Vs and on/off current ratio of 10^7 at a temperature of 250 °C. Hence, from our previous works [5–7,23,29], we propose a noncontact laser irradiation on sputter-deposited NiO_x/SiO_2-based TFTs as a potential technique to enhance the electrical parameters by tuning the laser fluence and a number of laser pulses. In this work, the relation between the number of laser pulses to the mobility of NiO_x, threshold voltage, on/off ratio and subthreshold swing of the NiO_x/SiO_2 TFT device is also studied extensively.

2. Device Fabrication Details

Nickel oxide films were deposited on SiO_2/Si substrate by reactive sputtering of 99.99% pure Ni target in an 80:20 oxygen–argon gas mixture at 300 °C. The cleaning procedure for the substrate is as follows: wash in cleaning solution (Micro-90), thoroughly rinse with DI water and conduct an ultra-sonication bath in methanol and ethanol for about 20 min. Simultaneously, the surfaces are dry-blown with nitrogen. The thickness of the films was found to be about 100 nm using spectroscopic ellipsometry studies [29]. Figure 1 depicts the layered structure of the NiO_x-based TFT. The gate metal (sputter-deposited Ni film of a thickness of 50 nm is deposited on the Si substrate (0.5 mm)). Then, an SiO_2 layer of thickness 200 nm is sputter-deposited by step-projection masking. Now, the NiO film of thickness 100 nm is deposited by reactive sputtering of Ni in 20% oxygen atmosphere. Post-deposition, the NiO layer is subjected to an Nd:YAG laser irradiation laser with a fourth harmonic wavelength λ = 266 nm and optimized laser fluence (smoothening of the film due to localized melting) of 150 mJ/cm^2 for different numbers of pulses (Figure 2a–d). At laser fluences slightly above and below the optimum laser fluence (i.e., 175 mJ/cm^2

and 125 mJ/cm^2, respectively), a marginal discontinuity (assumed to be a microhole) in the film can be observed at the center of the laser spot. This may arise due to a slight nonuniformity in the thickness of the sputter-deposited NiO film. The laser fluence is kept below a threshold (200 mJ/cm^2) for any observable physical damage/ablation. Finally, the source and drain metal (Al film of thickness 50 nm) are deposited by RF sputtering. The mobility was obtained using a Hall effect measurement setup at room temperature with a magnetic field of 2500 G [29]. The polycrystalline structure of the as-deposited NiO_x is verified on a Rigaku X-ray diffractometer with Cu K_a radiation (λ = 0.154 nm) and a Ni filter.

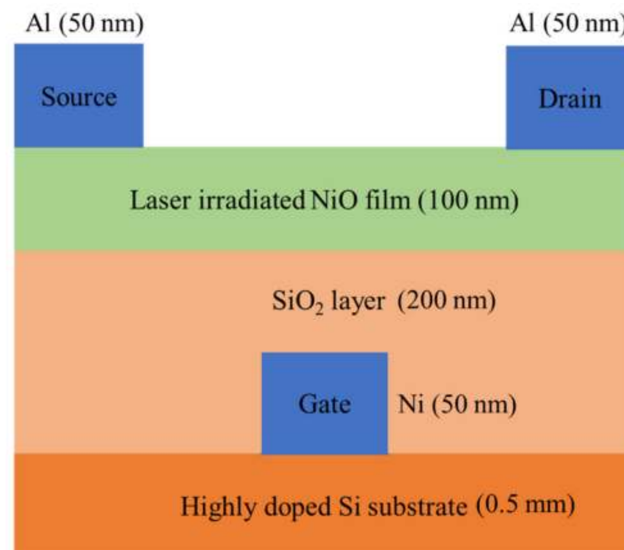

Figure 1. Layered structure of laser-irradiated NiO_x-based TFT (Staggered bottom gate TFT).

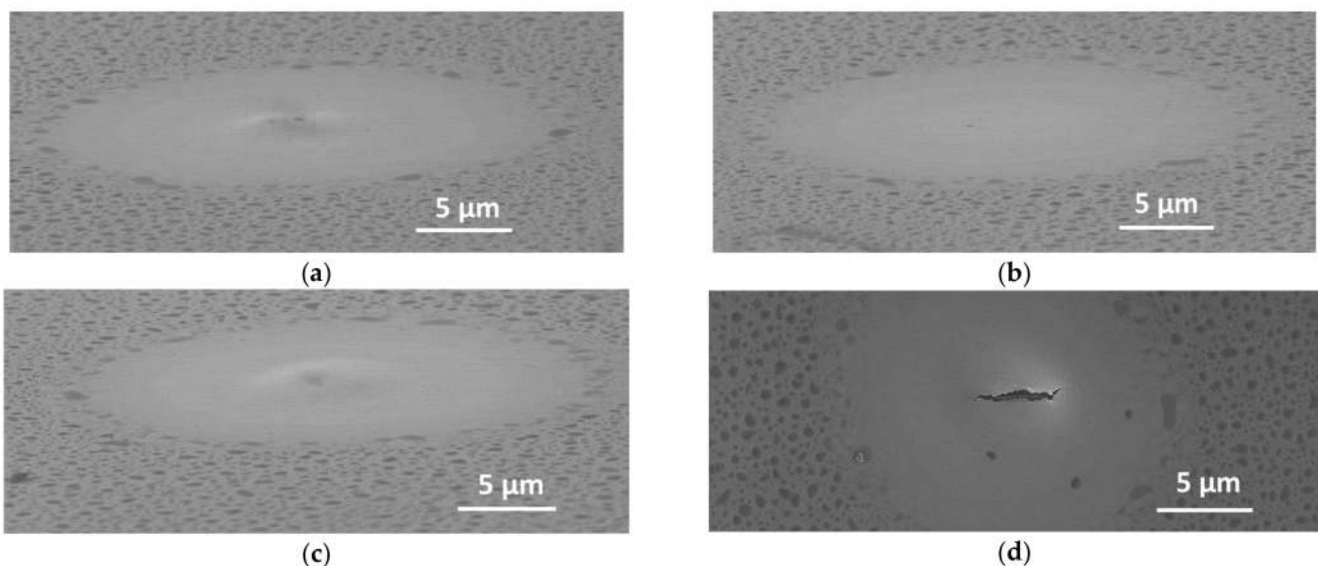

Figure 2. Scanning Electron Microscope images of laser-irradiated NiO_x/SiO_2 TFT (Scale: 1 inch = 10 µm). (**a**) Laser fluence of 125 mJ/cm^2, (**b**) 150 mJ/ cm^2, (**c**) 175 mJ/ cm^2 and (**d**) 200 mJ/ cm^2.

3. Results and Discussion

Figure 3a depicts the relationship between the mobility and the number of laser pulses. The mobility is affected by several scattering mechanisms, including lattice vibrations, ionized impurities, grain boundaries, interface surface roughness, lattice strain and other

structural defects, velocity saturation and electron trapping [41]. The field-effect mobility, which is the most widely used parameter to evaluate the TFT performance, gradually increases from 1.25 cm^2/V-s to 3 cm^2/V-s as the number of laser pulses increases in steps of 100 pulses to 500 pulses, after which, from 600 pulses to 1000 pulses, the hole concentration ceases to increase. This is now reflected in the mobility, decreasing to about 2.5 cm^2/V-s and finally reaching a value of 2.4 cm^2/V-s.

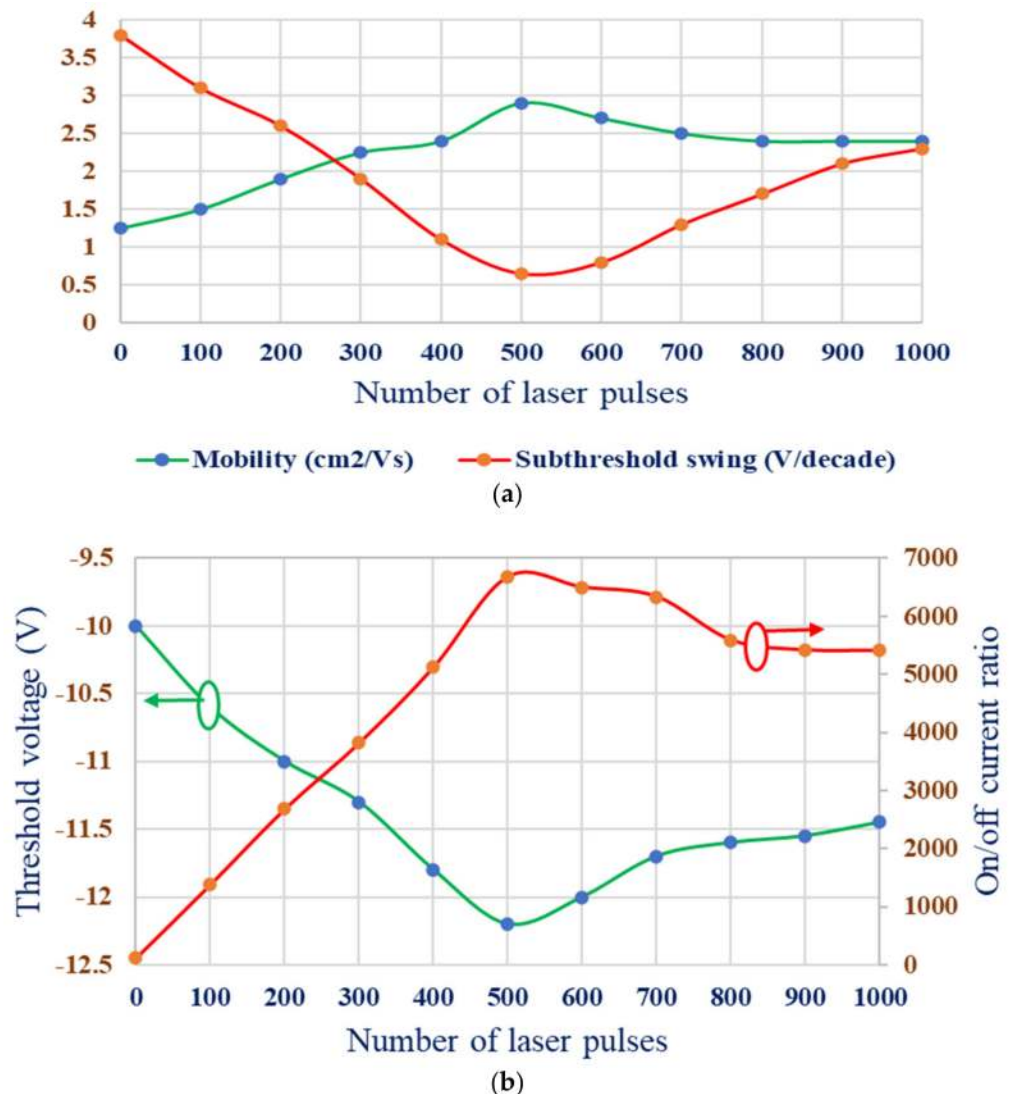

Figure 3. Dependence of number of laser pulses on (**a**) mobility (cm^2/V-s), subthreshold swing (V/decade) and (**b**) on/off current ratio, threshold voltage (V).

Similarly, the subthreshold swing (SS) is an important parameter that indicates the switching efficiency of a transistor. The SS is directly related to the quality of the dielectric/semiconductor interface. When the SS value is low, then the operation speed is high, and the power consumption is also low. As the number of laser pulses increases from 0 to 500, the value of SS decreases from 3.8 to 0.65 V/decade (Figure 3a). After 500 pulses up to 1000 pulses, the SS starts to increase to 2 V/decade, which suggests that the NiO layer is now slowly reduced to an amorphous film from a polycrystalline film [29]. As a result, this change degrades the dielectric/semiconductor interface quality. Hence, from Figure 3a, it is evident that 500 laser pulses is the point where both the mobility and SS are tuned for an optimum performance of NiO TFT.

Figure 3b represents the relationship between the on/off current ratio and the number of laser pulses. The on/off current ratio I_{on}/I_{off} is extracted from the transfer characteristic

curve. If the number of laser pulses increases from 0 to 500, then the ratio value constantly increases to 6.5×10^4. For 600 to 1000 laser pulses, the formation of Ni-rich NiO [29] results in a relatively lower mobility, thus reducing the on/off current ratio from 6.5×10^4 to 5.5×10^4.

Figure 3b also establishes the relationship between the threshold voltage and the number of laser pulses. The threshold voltage (V_{TH}) is the measure of how well the channel is formed near the dielectric layer/active layer interface in TFTs. Depending on the values of V_{TH} being negative or positive, the p-type TFT devices typically operate in enhancement or depletion modes, respectively. As the number of laser pulses increases from 0 to 500, the value of the threshold voltage decreases to −12.5 V. This is attributed to the increase in the carrier concentration of NiO. For 600 to 1000 laser pulses, as the carrier concentration stabilizes, the V_{TH} also stabilizes and reaches a value of −11.5 V. Table 1 presents a comparison of the electrical parameters reported in this work with previously reported NiO TFTs.

Table 1. Comparison of reported works on p-type NiO TFTs with the present work.

Ref.	Published Year	Oxide Layer	Mobility (cm^2/V-s)	Subthreshold Swing (V/decade)	On/off Current Ratio	Threshold Voltage (V)
[42]	2013	NiO	5.20	3.91	2.2×10^3	-
[43]	2015	NiO	0.05	2.6	10^3	8.6
[44]	2016	Sn:NiO_x	0.97	0.24	10^6	1.44
[45]	2017	Cu:NiO_x	1.53	0.13	3×10^4	0.45
This work	2021	NiO_x	3.00	0.65	6.5×10^4	−12.5

Furthermore, the associated $(I_{DS})^{\frac{1}{2}}$ and I_{GS} as a function of the V_{GS} are shown in Figure 4a–c. It was found that the saturation drain-source current and the gate leakage current were −40 µA and −8 nA, respectively, when the p-type NiO TFTs operated at a V_{DS} of −10 V and a V_{GS} of −9 V. The associated on-to-off current ratio was 6.5×10^4. The associated threshold voltage and subthreshold swing were −8 V and 0.56 V/decade, respectively.

The output characteristics of the p-type NiO-based TFT are divided into two main operating regions depending on the value of V_{DS}: linear and saturation regions. In the linear region, V_{GS} controls the channel resistance, thus accumulating charges uniformly in the channel. In the saturation region, for a constant V_{GS}, I_{DS} is constant, which suggests a lack of channel region due to a depletion of charges in the accumulation layer. For the 500 pulses laser-irradiated NiO_x/SiO_2 TFT, the output characteristics are shown in Figure 5.

At a constant V_{GS} of 0 V, when the voltage V_{DS} decreases from 0 V to −20 V, the value of the current I_{DS} decreases from 0 µA to −1.6 µA. At a constant V_{GS} of −3 V, when the voltage V_{DS} decreases from 0 V to −20 V, the value of the current I_{DS} decreases from 0 µA to −3 µA. At a constant V_{GS} of −6 V, when the voltage V_{DS} decreases from 0 V to −7.5 V, the value of the current I_{DS} decreases from 0 µA to −15 µA and remains constant up to −20 V. Again, at a constant V_{GS} of −9 V, when voltage V_{DS} decreases from 0 V to −10 V, the value of the current I_{DS} decreases from 0 µA to −40 µA and remains constant up to −20 V.

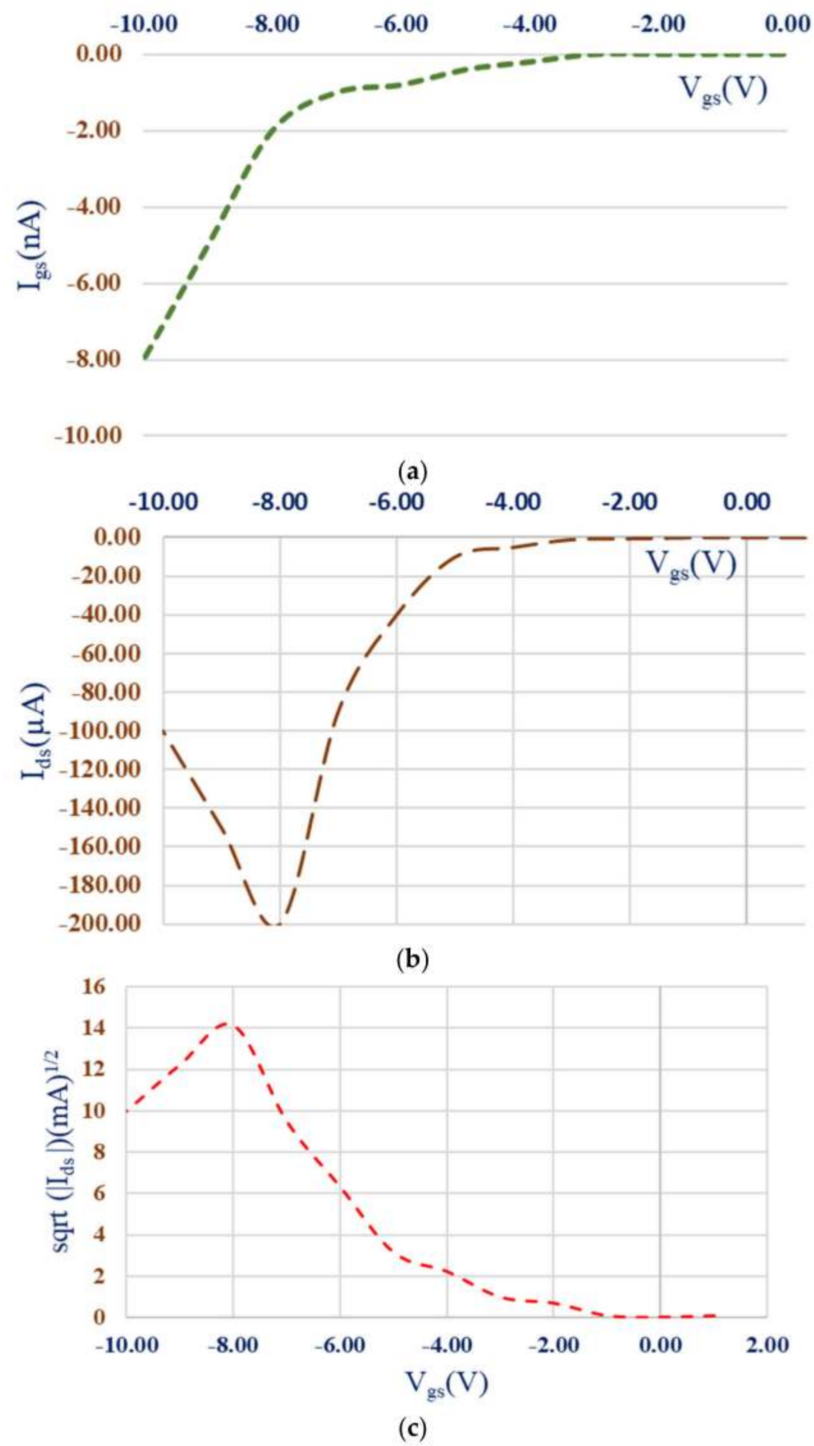

Figure 4. (**a**) Gate-source current, (**b**) Drain-source current and (**c**) transconductance as a function of the gate-source voltage (Transfer characteristics) of the p-type NiO thin-film transistor.

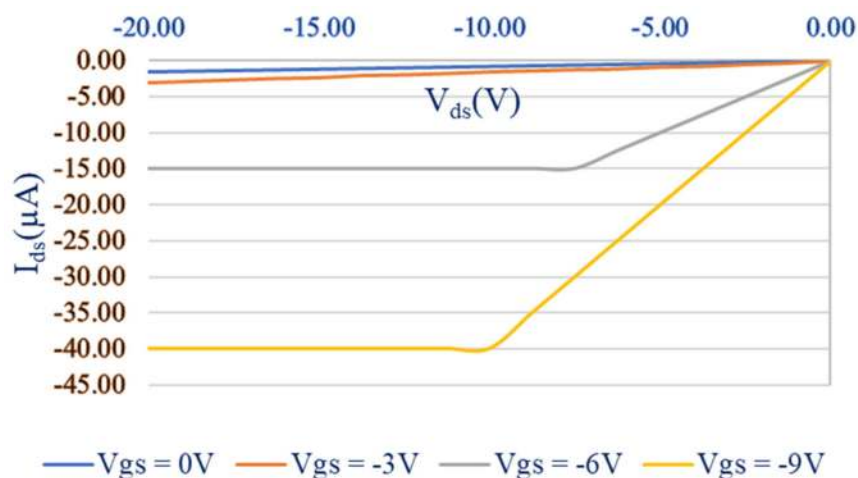

Figure 5. Drain source current-drain source voltage characteristics of the NiO TFT.

4. Conclusions

In this work, we studied the effects of laser irradiation in enhancing the electrical performance of p-type NiO_x TFT with SiO_2 as a high-k dielectric layer. The mobility increased from 1.25 cm^2/V-s for the as-deposited NiO_x thin film to 3 cm^2/V-s for the 500 laser pulse-irradiated sample. Similar enhancements were observed for the laser-irradiated sample in terms of the threshold voltage, subthreshold swing and the on/off current ratio. The plausible mechanism responsible for the reported phenomenon was that the excess energy the charge carriers possess, combined with the very high light intensity, resulted in a complex defect/interstitial tuning (Ni/O defect formations), thus enhancing the electrical performance of the TFT.

Author Contributions: Conceptualization, P.M., S.I.; methodology, S.I., S.S.; software, J.K.R.; validation, P.M., S.I.; formal analysis, P.M., J.K.R.; investigation, S.I., S.S.; resources, S.I.; data curation, J.K.R..; writing—original draft preparation, P.M., S.I.; writing—review and editing, S.I., S.S.; visualization, J.K.R. All authors have read and agreed to the published version of the manuscript.

Funding: This research received no external funding.

Institutional Review Board Statement: Not applicable.

Informed Consent Statement: Not applicable.

Data Availability Statement: Not applicable.

Acknowledgments: The authors would like to thank the department of Electrical Engineering and Computer Science (EECS) and the Center for Material Synthesis and Characterization (CMSC) at the University of Toledo for support to carry out this work.

Conflicts of Interest: The authors declare no conflict of interest.

References

1. Kim, H.J.; Park, K.; Kim, H.J. High-performance vacuum-processed metal oxide thin film transistors: A review of recent developments. *J. Soc. Inf. Disp.* **2020**, *28*, 591–622. [CrossRef]
2. Pattanasattayavong, P.; Mottram, A.D.; Yan, F.; Anthopoulos, T.D. Study of the Hole Transport Processes in Solution-Processed Layers of the Wide Bandgap Semiconductor Copper(I) Thiocyanate (CuSCN). *Adv. Funct. Mater.* **2015**, *25*, 6802–6813. [CrossRef]
3. Martins, R.F.P.; Ahnood, A.; Correia, N.; Pereira, L.M.N.P.; Barros, R.; Barquinha, P.M.C.B.; Costa, R.; Ferreira, I.M.M.; Nathan, A.; Fortunato, E.E.M.C. Recyclable, Flexible, Low-Power Oxide Electronics. *Adv. Funct. Mater.* **2013**, *23*, 2153–2161. [CrossRef]
4. Kim, S.Y.; Ahn, C.H.; Lee, J.H.; Kwon, Y.H.; Hwang, S.; Lee, J.Y.; Cho, H.K. p-Channel Oxide Thin Film Transistors Using Solution-Processed Copper Oxide. *ACS Appl. Mater. Interfaces* **2013**, *5*, 2417–2421. [CrossRef]
5. Khan, K.; Itapu, S.; Georgiev, D.G. Rectifying behavior and light emission from nickel oxide MIS structures. *MRS Adv.* **2016**, *1*, 3341–3347. [CrossRef]
6. Khan, K.; Itapu, S.; Georgiev, D.G. Negative differential resistance (NDR) behavior of nickel oxide (NiO) based metal-insulator-semiconductor structures. *J. Electron. Mater.* **2020**, *49*, 333–340. [CrossRef]

7. Borra, V.; Itapu, S.; Georgiev, D.G. Sn whisker growth mitigation by using NiO sublayers. *J. Phys. D Appl. Phys.* **2017**, *50*, 475309. [CrossRef]
8. Manders, J.R.; Tsang, S.W.; Hartel, M.J.; Lai, T.H.; Chen, S.; Amb, C.M.; Reynolds, J.R.; So, F. Solution-Processed Nickel Oxide Hole Transport Layers in High-Efficiency Polymer Photovoltaic Cells. *Adv. Funct. Mater.* **2013**, *23*, 2993–3001. [CrossRef]
9. Sato, H.; Minami, T.; Takata, S.; Yamada, T. Transparent conducting p-type NiO thin films prepared by magnetron sputtering. *Thin Solid Films* **1993**, *236*, 27–31. [CrossRef]
10. Chen, S.C.; Kuo, T.Y.; Sun, T.H. Microstructures, electrical and optical properties of non-stoichiometric p-type nickel oxide films by radio frequency reactive sputtering. *Surf. Coat. Technol.* **2010**, *205*, S236–S240. [CrossRef]
11. Chen, H.-L.; Lu, Y.-M.; Hwang, W.-S. Characterization of sputtered NiO thin films. *Surf. Coat. Technol.* **2005**, *198*, 138–142. [CrossRef]
12. Reddy, Y.A.K. Influence of Growth Temperature on the Properties of DC Reactive Magnetron Sputtered NiO Thin Films. *Int. J. Curr. Eng. Technol.* **2013**, *2*, 351–357. [CrossRef]
13. Subramanian, B.; Mohammed Ibrahim, M.; Murali, K.R.; Vidhya, V.S.; Sanjeeviraja, C.; Jayachandran, M. Structural, optoelectronic and electrochemical properties of nickel oxide films. *J. Mater. Sci. Mater. Electron.* **2009**, *20*, 953–957. [CrossRef]
14. Agrawal, A.; Habibi, H.R.; Agrawal, R.K.; Cronin, J.P.; Roberts, D.M.; CaronPopowich, R.; Lampert, C.M. Effect of deposition pressure on the microstructure and electrochromic properties of electron-beam-evaporated nickel oxide films. *Thin Solid Films* **1992**, *221*, 239–253. [CrossRef]
15. Yeh, W.; Matsumura, M. Chemical Vapor Deposition of Nickel Oxide Films from Bis-π-Cyclopentadienyl-Nickel. *Jpn. J. Appl. Phys.* **1997**, *36 Pt 1*, 6884–6887. [CrossRef]
16. Guo, W.; Hui, K.N.; Hui, K.-S. High conductivity nickel oxide thin films by a facile sol-gel method. *Mater. Lett.* **2013**, *92*, 291–295. [CrossRef]
17. Tanaka, M.; Mukai, M.; Fujimori, Y.; Kondoh, M.; Tasaka, Y.; Baba, H.; Usami, S. Transition metal oxide films prepared by pulsed laser deposition for atomic beam detection. *Thin Solid Films* **1996**, *281–282*, 453–456. [CrossRef]
18. Reguig, B.A.; Khelil, A.; Cattin, L.; Morsli, M.; Bernède, J.C. Properties of NiO thin films deposited by intermittent spray pyrolysis process. *Appl. Surf. Sci.* **2007**, *253*, 4330–4334. [CrossRef]
19. Kang, J.-K.; Rhee, S.-W. Chemical vapor deposition of nickel oxide films from $Ni(C_5H_5)_2O_2$. *Thin Solid Films* **2001**, *391*, 57–61. [CrossRef]
20. Liu, H.; Zheng, W.; Yan, X.; Feng, B. Studies on electrochromic properties of nickel oxide thin films prepared by reactive sputtering. *J. Alloys Compd.* **2008**, *462*, 356–361. [CrossRef]
21. Bruckner, W.; Kaltofen, R.; Thomas, J.; Hecker, M.; Uhlemann, M.; Oswald, S.; Elefant, D.; Schneider, C.M. Stress development in sputtered NiO thin films during heat treatment. *J. Appl. Phys.* **2003**, *94*, 4853. [CrossRef]
22. Kuzmin, A.; Purans, J.; Rodionov, A. X-ray absorption spectroscopy study of the Ni K edge in magnetron-sputtered nickel oxide thin films. *J. Phys. Condens. Matter* **1997**, *9*, 6979–6993. [CrossRef]
23. Itapu, S.; Borra, V.; Mossayebi, F. A computational study on the variation of bandgap due to native defects in stoichiometric NiO and Pd, Pt doping in stoichiometric NiO. *Condens. Matter* **2018**, *3*, 46. [CrossRef]
24. Moening, J.P.; Georgiev, D.G. Formation of conical silicon tips with nanoscale sharpness by localized laser irradiation. *J. Appl. Phys.* **2010**, *107*, 14307. [CrossRef]
25. Moening, J.P.; Thanawala, S.S.; Georgiev, D.G. Formation of high-aspect-ratio protrusions on gold films by localized pulsed laser irradiation. *Appl. Phys. A* **2009**, *95*, 635–638. [CrossRef]
26. Lu, H.; Tu, Y.; Lin, X.; Fang, B.; Luo, D.; Laaksonen, A. Effects of laser irradiation on the structure and optical properties of ZnO thin films. *Mater. Lett.* **2010**, *64*, 2072–2075. [CrossRef]
27. Kim, K.; Kim, S.; Lee, S.Y. Effect of excimer laser annealing on the properties of ZnO thin film prepared by sol-gel method. *Curr. Appl. Phys.* **2012**, *12*, 585–588. [CrossRef]
28. Gupta, P.; Dutta, T.; Mal, S.; Narayan, J. Controlled p-type to n-type conductivity transformation in NiO thin films by ultraviolet-laser irradiation. *J. Appl. Phys.* **2012**, *111*, 13706. [CrossRef]
29. Itapu, S.; Georgiev, D.G.; Uprety, P.; Podraza, N.J. Modification of reactively sputtered NiO_x thin films by pulsed laser irradiation. *Phys. Status Solidi (A)* **2017**, *214*, 1600414.
30. Abal'oshev, A.; Abal'osheva, I.; Gierłowski, P.; Lewandowski, S.J.; Konczykowski, M.; Rizza, G.; Chromik, Š. Effect of pulsed UV laser irradiation on the properties of crystalline $YBa_2Cu_3O_{7-\delta}$ thin films. *Supercond. Sci. Technol.* **2007**, *20*, 433–440. [CrossRef]
31. Chang, L.; Jiang, Y.; Ji, L. Improvement of the electrical and ferromagnetic properties in $La_{0.67}Ca_{0.33}MnO_3$ thin film irradiated by CO_2 laser. *Appl. Phys. Lett.* **2007**, *90*, 82505. [CrossRef]
32. Ji, L.; Jiang, Y.; Wang, W.; Yu, Z. Enhancement of the dielectric permittivity of Ta_2O_5 ceramics by CO_2 laser irradiation. *Appl. Phys. Lett.* **2004**, *85*, 1577–1579. [CrossRef]
33. Papernov, S.; Kozlov, A.A.; Oliver, J.B.; Kessler, T.J.; Shvydky, A.; Marozas, B. Near-ultraviolet absorption annealing in hafnium oxide thin films subjected to continuous-wave laser radiation. *Opt. Eng.* **2014**, *53*, 122504. [CrossRef]
34. Scorticati, D.; Illiberi, A.; Bor, T.; Eijt, S.W.H.; Schut, H.; Römer, G.R.B.E.; De Lange, D.F. Annealing of SnO_2 thin films by ultra-short laser pulses. *Opt. Express* **2014**, *22*, A607. [CrossRef]
35. Ichikawa, Y.; Chi, H.A.; Setsune, K.; Kawashima, S.I.; Kugimiya, K. Crystallization of Amorphous Titanium Oxide Thin Films by Pulsed UV-Laser Irradiation. *MRS Proc.* **1995**, *397*, 447. [CrossRef]

36. Farooq, W.A.; Al Saud, M.; Alahmed, Z.A. Structural and optical properties of laser irradiated nanostructured cadmium oxide thin film synthesized by a sol-gel spin coating method. *Opt. Spectrosc.* **2016**, *120*, 745–750. [CrossRef]
37. Hong, R.; Wei, C.; He, H.; Fan, Z.; Shao, J. Influences of CO_2 laser irradiation on the structure and photoluminescence of zinc oxide thin films. *Thin Solid Films* **2015**, *485*, 262–266. [CrossRef]
38. Liu, A.; Liu, G.; Zhu, H.; Shin, B.; Fortunato, E.; Matins, R.; Shan, F. Hole mobility modulation of solution-processed nickel oxide thin-film transistor based on high-k dielectric. *Appl. Phys. Lett.* **2016**, *108*, 233506. [CrossRef]
39. Shan, F.; Liu, A.; Zhu, H.; Kong, W.; Liu, J.; Shin, B.; Fortunato, E.; Martins, R.; Liu, G. High-mobility p-type NiO_x thin-film transistors processed at low temperatures with Al_2O_3 high-k dielectric. *J. Mater. Chem. C* **2016**, *4*, 9438–9444. [CrossRef]
40. Xu, W.; Zhang, J.; Li, Y.; Zhang, L.; Chen, L.; Zhu, D.; Cao, P.; Liu, W.; Han, S.; Liu, X.; et al. p-type transparent amorphous oxide thin-film transistors using low-temperature solution-processed nickel oxide. *J. Alloys Compd.* **2019**, *806*, 40–51. [CrossRef]
41. Shang, Z.W.; Hsu, H.H.; Zheng, Z.W.; Cheng, C.H. Progress and challenges in p-type oxide based thin film transistors. *Nanotechnol. Rev.* **2019**, *8*, 422–443. [CrossRef]
42. Jiang, J.; Wang, X.H.; Zhang, Q.; Li, J.Q.; Zhang, X.X. Thermal oxidation of Ni films for p-type thin-film transistors. *Phys. Chem. Chem. Phys.* **2013**, *15*, 6875. [CrossRef]
43. Chen, Y.; Sun, Y.; Dai, X.; Zhang, B.; Ye, Z.; Wang, M.; Wu, H. Tunable electrical properties of NiO thin films and p-type thin-film transistors. *Thin Solid Films* **2015**, *592*, 195–199. [CrossRef]
44. Lin, T.; Li, X.; Jang, J. High-performance p-type NiO_x thin-film transistor by Sn doping. *Appl. Phys. Lett.* **2016**, *108*, 233503. [CrossRef]
45. Lin, A.; Zhu, H.; Guo, Z.; Meng, Y.; Liu, G.; Fortunato, E.; Martins, R.; Shan, F. Solution combustion synthesis: Low-temperature processing of p-type Cu:NiO thin films for transparent electronics. *Adv. Mater.* **2017**, *29*, 1701599.